International Academic Institute for Science and Technology

International Academic Journal of Science and Engineering
Vol. 6, No. 1, 2019, pp. 1-14.

ISSN 2454-3896

International Academic Journal of Science and Engineering

www.iaiest.com

Probabilistic Quantitative Precipitation Forecasting Using Machine Learning Methods and Probable Maximum Precipitation

Xaniyar Asgari-Motlagh[a], Mehdi Ketabchy[b,c], Ali Daghighi[d]

[a]*Department of Civil & Environmental Engineering, Amirkabir University of Technology, Tehran, 158754413, Iran*

[b]*Department of Biological System Engineering, Virginia Polytechnic Institute and State University, Blacksburg, 24061, U.S.A.*
[c]*Transportation Business Line, Gannett Fleming, Inc., Fairfax, VA, United States*

[d]*Department of Computer Engineering and Information Technology, Amirkabir University of Technology, Tehran, 158754413, Iran*

Abstract

Precise prediction of rainfall, especially in dry and semidry regions, can play a significant role in effective management of water resources. The recent challenging problems in management of water resources and dealing with climatic risks is finding an accurate forecasting method. Although extensive research has been conducted in employing computational intelligence methods to predict precipitation and runoff, the probable maximum precipitation (PMP) method is one of the more practical tools used to design water structures and predict maximum floods in Iran. In this study the efficiency of this method compared to using artificial neural network methods has been challenged. The results show while an artificial neural network method will produce an accurate response for predicting precipitation processes, yielding a very high correlation coefficient of about 97%, a synoptic method will estimate maximum values far better than does the neural network approach. Concurrent use of these two methods will result in the most satisfactory investigation and comparison as well as the most useful modeling.

Keywords: Probable Maximum Precipitation (PMP), Artificial Neural Network (ANN), Water resources management, Predict maximum floods

DOI:10.9756/IAJSE/V6I1/1910001
Received: 05 March 2019/Revised: 02 April 2019/Accepted: 06 May 2019/Published: 28 June 2019

Introduction

Having precise information about future precipitation is crucial for management of reservoirs of dams and controlling floods, and precipitation has a huge influence on traffic, wastewater drainage system, and other human activities in urban societies (Ketabchy, et al., 2018; Nikoo, et al., 2017). Precipitation is one of the most complex and random natural phenomena, and the effects of both predictible and unpredictible factors are so great that it has changed from a clear systematic phenomenon to a complex and chaotic structure (Danco, et al., 2016; Yazdi, et al., 2016; Daghighi, et al., 2017), so decision-makers, especially water resources managers, increasingly require a more reliable prediction method for management decision-making (Nahvi, et al., 2018). Prediction of precipitation over the past decades has remained a great challenge among hydrologic issues in spite of the volume of previous work, because climate and precipitation are highly nonlinear and complex phenomena that necessitate advanced computational modeling and simulation for precise prediction (Zodrow, et al., 2017). Due to the nonlinear nature of models based on artificial neural networks and their closer correspondence with the nature of stochastic phenomena, such models have been under extensive use in recent years across various scientific areas, including hydrology (Haghiri, et al., 2018; Daghighi, 2017). The first work in precipitation-runoff modeling using artificial neural networks was performed by Hsu, et al. (1995) and Tokar, et al (1999). They concluded that use of artificial intelligence based methods can, to a large extent, eliminate most defects in conceptual and data-oriented methods (Anctil & Tape, 2004). They conducted a comparative study to predict the discharge of a future day's flow for two basins using the multiple functions of neurons in an artificial neural network and the hybrid function of a neural network-wavelet system.

Partal and Kişi (2007) employed the wavelet-neural-fuzzy hybrid method for predicting precipitation at three synoptic stations in Turkey using a combination of discrete wavelet transform and fuzzy artificial network methods. They converted the daily observed precipitation into a subseries using discrete wavelet transforms, then employed the subseries as input to fuzzy neural models for predicting daily precipitation. Rajaee, et al., (2010) utilized ANN, neural-fuzzy, multiple regression, and intensity-precipitation traditional curve methods to model the time series of concentration of sediments suspended at a river and measurement station for a basin in the US.

Kisi, et al., (2013) employed gene expression programming and coefficient of efficiency and scatter index to determine the best combination of inputs of variables for modeling precipitation runoff from a small catchment in Turkey using an artificial neural network and an adaptive neuro-fuzzy inference system. Based on data from the National Oceanic and Atmospheric Administration (NOAA), Kagan, et al., (1973) dealt with a brief description of probable maximum precipitation (PMP) computational methods for non-mountainous and mountainous regions as well as for regions without meteorological data. Legates, et al., (1999) described new concepts and their uses in PMP estimation and offered suggestions about a modified method used in assessment of PMP magnitude.

Using the periodicity general equation and the statistics of daily precipitation of over 2600 stations, 90% located within the US, Hershfield (1961) found that K=15 is a push curve for observed data of maximum daily precipitation. In another study, Rosso (2006) observed that the K value inversely changes with the mean maximum daily precipitation, and a K value of 15 is very large for high-precipitation regions but very low for dry regions. In 1961, he calculated the K value by further analyzing 24-hour, 1-hour, and 5-min continuities, and increased its value from those previously described (Hershfield, 1961), and based on re-examining 6-hour precipitations, he changed the K value.

The aim of this study is to predict precipitation and runoff in the Tehran region using two methods, one based on field data, the other based on advanced and artificial intelligence methods. A synoptic method extensively used in applied projects will be used on the field data, while an artificial neural network modeling method will be used as an example of the artificial intelligence approach.

Material and Methods

Feed-Forward networks are among the most common architectures of Back-Propagation networks that often use one or several hidden layers with sigmoid neurons along with a final linear layer (Mishra & Desai, 2006; Farajzadeh, et al., 2014; Pradhan & Lee, 2010; Chang & Chao, 2006). The inclusion of several layers of neurons with a nonlinear transfer function allows the network the capability of learning both linear and nonlinear relationships between inputs and outputs. The output linear layer permits the network to have an output outside the range of [-1,+1], and this network can be used to estimate each function with a limited number of discontinuities.

The algorithm used in neural networks is the Levenberg-Marquadt algorithm. As with pseudo-Newtonian methods, this algorithm tries to reduce computations by avoiding calculation of a Hessian matrix. When the efficiency function is in sum-of-squares form (typical in Feed-Forward networks), the Hessian matrix can be calculated following Eq. (1):

$$H = J^T J \,, \tag{1}$$

The slope can also be calculated using Eq. (2):

$$g = J^T e \,, \tag{2}$$

where J is the Jacobian matrix consisting of first derivatives of network errors in relation to weights and biases, and e is the error vector of the network. The Jacobian matrix can be calculated using standard back-propagation techniques, and its complexity is far less than that of the Hessian matrix. The Levenberg-Marquadt algorithm uses Eq. (3) to calculate an approximation to the Hessian matrix:

$$X_{k+1} = X_k - [J^T J - \mu I\,] J^T e \,, \tag{3}$$

When the numerical value of μ is zero, this transfer function becomes similar to the Newtonian method with Hessian matrix approximation, but when μ is large, this method changes into the conjugate gradient method with small steps. Since the Newtonian method is more accurate than the conjugate gradient method, μ declines after each successful step (successful step corresponds to reduction of the efficiency function), it grows only when the experimental step increases the efficiency function. In this way, each iteration always decreases the efficiency function. Both the number of neurons in the hidden layer and the output were chosen based on trial and error, as was the optimal structure of the artificial neural networks. The aim of this trial and error approach was to determine the number of neurons in the hidden layer and the number of algorithm iterations. This procedure can use either the nntool toolbox in MATLAB software or relevant coding. In this study, the number of iterations was determined as 10-500 based on trial and error. To achieve great convergence power in training ANN networks, a Levenberg-Marquadt algorithm was used. In this study, the sigmoid tangent transfer function has been found to be beneficial as the nonlinear kernel of neural networks. To train the network model, 70% of data was chosen, while the

remaining 30% was employed for validation. Note that, for prediction by ANN, delay of precipitation data and discharge has been chosen as the input.

The maximum precipitation height meteorologically possible for a specific period of time in a special region is called the PMP, the basis for designing many water projects. Desirable determination of PMP is based on synoptic methods, with reliance on statistics and extensive information being one of its limitations. For this reason, statistical methods have been developed that accomplish PMP calculations from only maximum precipitation statistics.

The method for determining the PMP in a basin involves the following five important steps:

1) Find altitude-continuity-level curves where PMP has been determined for the level and continuity of a certain shower.
2) Determine a standard isohyetal pattern in which the precipitation is distributed spatially in an oval shape.
3) Determine a navigation modification factor if the longitudinal axis of the standard isohyetal pattern has not been determined along the atmospheric humidity flow in the region, resulting in PMP underestimation.
4) Determine the critical shower level resulting in the maximum PMP in the basin.
5) Determine a isohyetal modification factor that in turn determines the PMP altitude percentage.

The position of stations has been detected both inside and around the basin. To plot the isohyetal lines, based on precipitation gradient equation, the relevant altitude was calculated for each specific value of precipitation, then isohyetal curves were plotted using ArcGIS software. Specifically, because the region was mountainous, isohyetal lines followed contour lines.

The assessment criterion

To align the type and range of data, normalization using Eq. (4) was used, resulting in a data range of [0,1] (Alvisi, et al., 2006):

$$x_N = \frac{x_i - x_{\min}}{x_{\max} - x_{\min}}, \tag{4}$$

where x_N is the normalized value and x_i is the variable value, with x_{min} and x_{max} the minimum and maximum values of the data. One of the main reasons for normalization is to make the model applicable for inputs with different dimensions; in this method, the inputs become dimensionless. Furthermore, significant numerical differences in different variables is resolved through normalization, and the range of the input data as precipitation and runoff becomes similar within the range [0,1].

In this study, to evaluate the efficiency of the models, the Determination Coefficient (DC) and the Root Mean Square Error (RMSE) have been calculated using Eq. (5), and Eq. (6):

$$DC = 1 - \frac{\sum_{i=1}^{n}(y_i - x_i)^2}{\sum_{i=1}^{n}(y_i - \overline{y_i})^2}, \tag{5}$$

$$RMSE = \sqrt{\frac{\sum_{i=1}^{n}(y_i - x_i)^2}{n}}, \quad (6)$$

where y_i is the data related to the model computation, x_i represents the observed data, $\bar{x}$ and $\bar{y}$ show the mean values of the data, and n denotes the number of data. DC is a criterion used for precise estimation of the model by comparing observed and computational data. $RMSE$ is a criterion typically used for determining differences between observed data and computational results generated by the model. The closer to 1 the DC value obtained based on normal data and the closer to zero the $RMSE$ value, the better the model's performance.

Case Study

This basin is located in the southern domain of central Tehran at 51.3890° eastern longitude and 35.6892° northern latitude. Its maximum altitude is 4000 m in the north, and its lowest altitude is 1320 m below the dam area. The average altitude of the basin is 1600 m above sea level, and approximately 61% of its area is situated at an altitude abover 2500 m above sea level. The total area of the basin is 845 km^2 (Mahmoudpour, et al., 2016).

Because this basin is invaded by pluvial systems from northern regions of Tehran slopes, the stations of interest are Geophysic, Mehr Abad, and Dushan Tappe synoptic stations selected from the northern Tehran plain and shown in Figure 1. Based on periodic investigations in this basin and previous maximum precipitation levels in the region, three pervasive storms were chosen as follows:

a) the storm on March 1991 with a 48-hour continuity
b) The storm on Nov 1994 with a 48-hour continuity
c) The storm on March 1996 with a 48-hour continuity

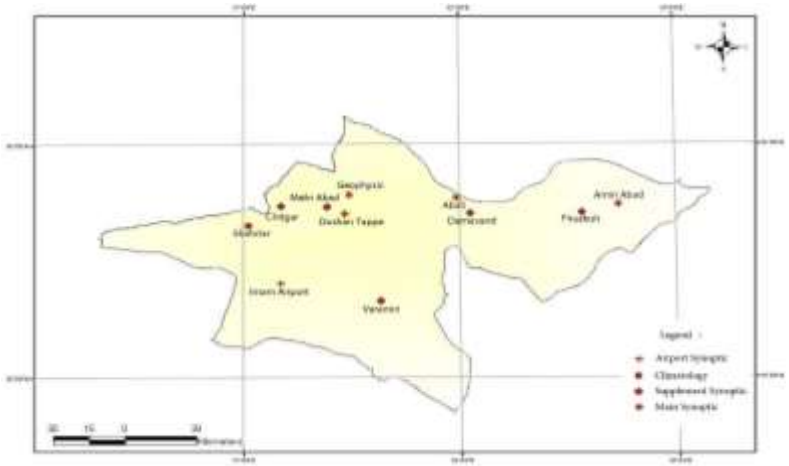


Figure 1: The logo of Copernicus Publications.

Results and Discussion

Before plotting isohyetal lines, since the correlation between precipitation and altitude was significant across the three studied storms, the area between the isohyetal lines was calculated, and based on this calculation, the volume of the water precipitated in each level could be estimated. It can be observed that in this basin, altitude affects precipitation and follows it. Using the isohyetal curves, tables of altitude, area, and isohyetal lines can be completed based on the areas studied, and Tables 1 – 3 shows details for the three major storms.

Table 1. The altitude and area of isohyetal lines on March 1991

Precipitation between the two isohyetal lines	Average of precipitation between the two isohyetal lines	The area between the two isohyetal lines	Volume of the precipitation between the two isohyetal lines	Cummulative area	Cummulative volume of the precipitation	The average of the precipitation
mm	mm	km^2	$m^3 \times 10^6$	km^2	$m^3 \times 10^6$	mm
under 60	50	31.25	1.5625	31.25	1.5625	50
60-80	70	97.35	6.8145	128.6	8.377	65.13997
80-100	90	201.54	18.1386	330.14	26.5156	80.31623
100-120	110	301.52	33.1672	631.66	59.6828	94.48564
120-140	130	96.4	12.532	728.06	72.2148	99.18798
140-160	150	74.96	11.244	803.02	83.4588	103.9312
160	170	41.98	7.1366	845	90.5954	107.2135

Table 2. The altitude and area of isohyetal lines on Nov 1994

Precipitation between the two isohyetal lines	Average of precipitation between the two isohyetal lines	The area between the two isohyetal lines	Volume of the precipitation between the two isohyetal lines	Cummulative area	Cummulative volume of the precipitation	The average of the precipitation
mm	mm	km^2	$m^3 \times 10^6$	km^2	$m^3 \times 10^6$	mm
under 60	50	47.35	2.3675	47.35	2.3675	50
60-80	70	74.46	5.2122	121.81	7.5797	62.2256
80-100	90	108.24	9.7416	230.05	17.3213	75.29363
100-120	110	207.62	22.8382	437.67	40.1595	91.75749
120-140	130	198.28	25.7764	635.95	65.9359	103.6809
140-160	150	154.38	23.157	790.33	89.0929	112.7287
160	170	54.67	9.2939	845	98.3868	116.4341

Table 3. The altitude and area of isohyetal lines on March 1996

Precipitation between the two isohyetal lines	Average of precipitation between the two isohyetal lines	The area between the two isohyetal lines	Volume of the precipitation between the two isohyetal lines	Cummulative area	Cummulative volume of the precipitation	The average of the precipitation
mm	mm	km^2	$m^3 \times 10^6$	km^2	m 3 * 10^6	mm
under 80	70	21.95	1.5365	21.95	1.5365	70
80-100	90	142	12.78	163.95	14.3165	87.32235
100-120	110	158.54	17.4394	322.49	31.7559	98.47096
120-140	130	215.64	28.0332	538.13	59.7891	111.1053
140-160	150	120.43	18.0645	658.56	77.8536	118.2179
160-180	170	108.07	18.3719	766.63	96.2255	125.5175
180	190	78.37	14.8903	845	111.1158	131.498

To calculate te precipitable water, the best solution is obtained at the warmest saturation point. Note that since the dew point is not constant across the studies but changes under different precipitation conditions, the maximum 12-hour continuity of dew point was extracted for the first, second, and third 10-day intervals of each month over the statistical period for Mehrabad, Qazvin, Karaj, Ramsar, and Noshahr synoptic stations.

Because the statistical periods of different stations are not the same, the data were fitted using a normal distribution model and the maximum dew point temperature and wind speed were estimated with 12-hour continuity for 50- and 80-year return periods. After maximizing the dew-point temperature using the SKEW/T/P diagram, the mixing ratio was obtained at the intersection of dew point and storm, then converted into 1000's of m Bar. This operation was performed for all storms with 50- and 80-year return periods, as shown in Table 4 presents. A Moisture Parameter (MP) value was obtained by dividing the mixing ratio of a certain return period at a balance of 1000 hecto-pascal.

Table 4. Maximizing the dew point temperature and the mixing ratio at 1000 hecto-pascal level for the average of the three storms

Station	12-hour maximum peak of continuity of the storm	Converting the on surface temperature to 1000 hecto-pascal	mixing ratio		12-hour maximum peak of continuity of 50-years return period dew point	12-hour continuity of 50-years return period dew point conversion to 1000 hecto-pascal	mixing ratio		Moisture Parameter	12-hour maximum peak of continuity of 80-years return period dew point	12-hour continuity of 80-years return period dew point conversion to 1000 hecto-pascal	mixing ratio		Moisture Parameter
			on the earth	at 1000 hecto-pascal			on the earth	at 1000 hecto-pascal				on the earth	at 1000 hecto-pascal	
Dushan Tappe	10.0	15.3	9.1	11.8	13.2	18.5	11.0	13.5	1.32	14.1	19.5	10.9	13.4	1.41
Geophysic	10.1	15.5	9.5	12.4	13.6	19.0	11.4	14.0	1.35	14.2	19.6	11.1	13.7	1.41
Mehr Abad	9.6	14.7	8.9	11.6	12.9	18.1	10.9	13.4	1.34	14.1	19.5	10.9	13.4	1.47
Mean									1.34					1.43

The maximum wind speed with 12-hour continuity for each 10-day period of the month within the statistical period and for 50- and 80-year return periods was estimated using statistical distribution (Gampbell Type III), with results shown in Tables 4 and 5. WP is a wind parameter is obtained by dividing the maximized wind speed within a certain return period by the maximized wind speed of the storm.

Table 5. Maximizing the windspeed for the average of three storm

Station	The maximum wind speed with 12-hour continuity	The maximized wind speed with 50-years return period	The maximized wind speed with 80-years return period	The factor of maximum wind speed with 12-hour continuity with 50-years return period	The factor of maximum wind speed with 12-hour continuity with 80-years return period
Dushan Tappe	13	26.4	29.7	2.0	2.3
Geophysic	14	26.9	30.1	1.9	2.2
Mehr Abad	11	25.9	28.1	2.4	2.6
Mean				2.1	2.3

The storm factor is calculated following Eq. (7):

$$SF = MP \times WP, \quad (7)$$

where MP is the moisture perimeter, and WP is the wind perimeter. The maximum humidity and wind speed factors are applied individually in the mean precipitation value of each storm with 50- and 80-year return periods, and the calculated PMP values for the basin are shown in Tables 6 and 7.

Table 6. The basin's PMP estimation by synoptic method with a 50-year period

Date	The average of the precipitation	Storm factor	PMP
Dushan Tappe	107.22	2.68	287.42
Geophysic	116.1	2.59	300.38
Mehr Abad	131.49	3.16	416.02

Table 7. The basin's PMP estimation by synoptic method with a 80-year period

Date	The average of the precipitation	Storm factor	PMP
Dushan Tappe	107.22	3.22	345.39
Geophysic	116.1	3.02	350.94
Mehr Abad	131.49	3.75	493.35

Because the basin studied is located in a mountainous region, it is necessary to take the effect of the mountain terrain into account in determining \ the humidity modification factor. In this way, since dew-point temperature for the storm and for 50- and 80-year return periods in each storm are considered separately at 1000 hecto-pascal, using the tables determined by the World Meteorological Organization (WMO), the dew point temperatures of interest were obtained at 200 hecto-pascal. The same temperatures were then calculated at an altitude of 1600 m (the average altitude of the basin above sea level) and

subtracted from one another. The numbers obtained from the return periods were then divided by the number resulting from the storm, obtaining the mountain adjustment factor for each station in each storm. After these operations, the average values of the factors were calculated for 50- and 80-year return periods in, as shown in Tables 8 and 9, and the wind speed factor and eventually the mean precipitation value of the basin applied at a cumulative level.

Table 8. The basin's PMP estimation using mountain adjustment factor for the 50-year return period

Date	The average of the precipitation	The wind speed factor with 50-years return period	Moisture coefficient due to mountain	PMP
Dushan Tappe	107.22	1.38	1.09	161.28
Geophysic	116.1	1.19	1.74	240.39
Mehr Abad	131.49	1.49	1.42	278.20

Table 9. The basin's PMP estimation using mountain adjustment factor for the 80-year return period

Date	The average of the precipitation	The wind speed factor with 80-years return period	Moisture coefficient due to mountain	PMP
Dushan Tappe	107.22	1.51	1.17	189.42
Geophysic	116.1	1.31	1.82	276.80
Mehr Abad	131.49	1.63	1.54	330.06

PMP values can be extracted from this table. Since PMP estimation obtained using synoptic methods is more complete and accurate than other methods because they consider atmospheric parameters, the above results can be used for constructing and designing hydraulic structures.

The ANN model is expressed in terms of (n,m,k), with n, m, and k representing the number of neurons in the input layers, the hidden layer, and the output layer, respectively. n denotes the number of input variables and since in this thesis the only output variable is run-off, k has been taken as one (k=1). As previously explained, the best m value can be calculated through trial and error.

The extent of increase in efficiency criteria for basins with low efficiency using the previous method is significantly larger. In the first and third stations, where the modeling exhibited good correspondence with the first two methods, no significant change was observed, while the modeling improved significantly for the second basin. In other words, as long as a model with simple structure is able to model time series, more complex modeling produces no significant change in the quality of modeling and only increases the computational load.

From previous modeling, the best efficiency criterion was related to the second station and the worst was associated with the third station. The observed and computational time series of these three stations are plotted in Figures 2 through 4.

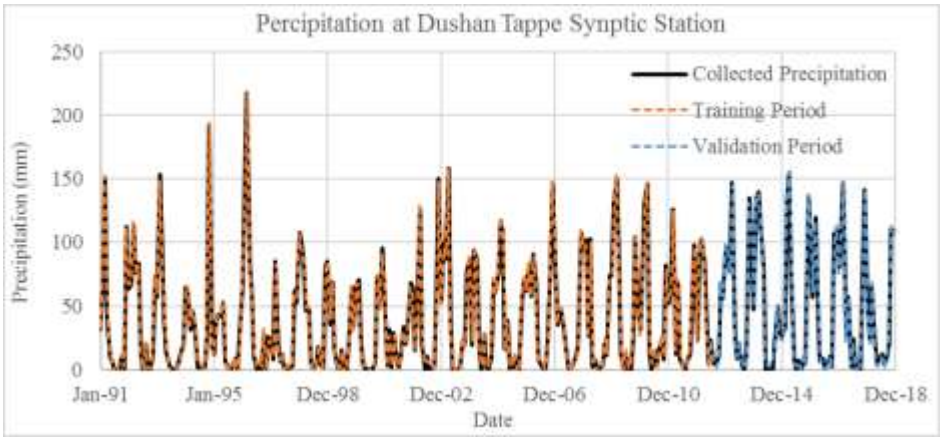


Figure 2: ANN modelling with training and validation period of Dushan Tappe station

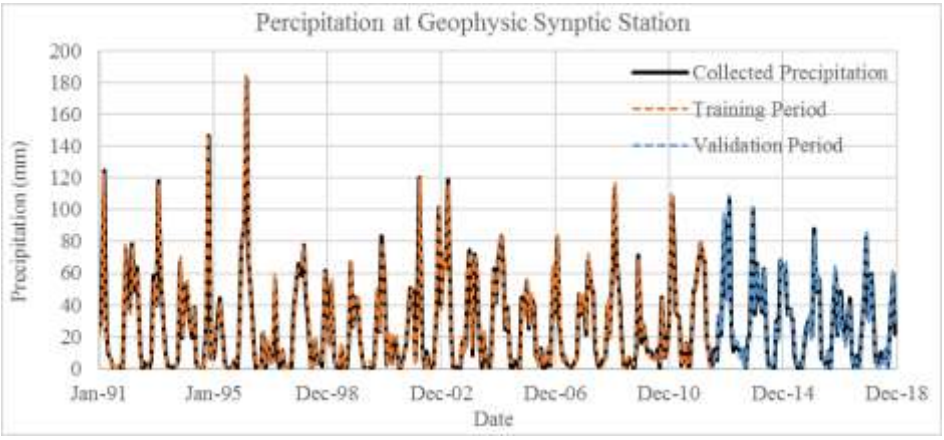


Figure 3: ANN modelling with training and validation period of Geophysic statio

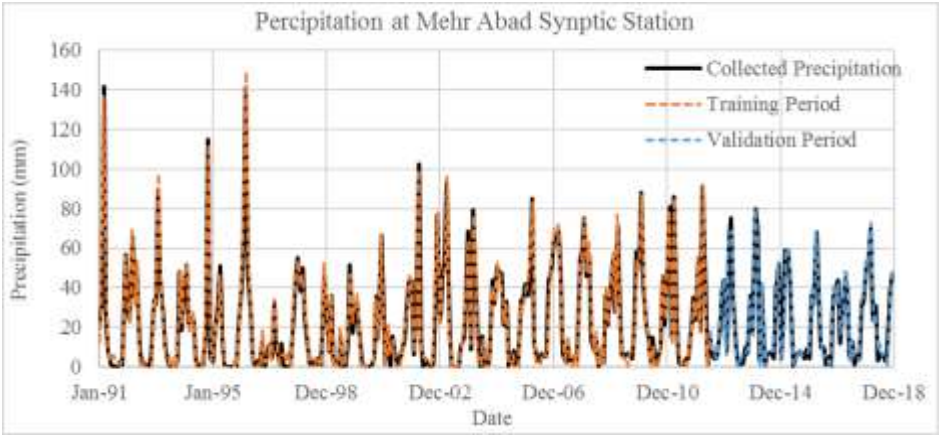


Figure 4: ANN modelling with training and validation period of Mehr Abad station.

All of the figures 2 to 4 reveal the results of neural network compared with the data from the training and validation activities. To obtain the maximum precipitation, the maximum point of each diagram should be obtained and individually calculated for each of the three stations. The important point when using an artificial neural network is that, in addition to determining the maximum, the results can be extracted throughout the entire time series. These values, based on diagram extraction, for the three stations at Dushan Tappe, Geophysic, and Mehr Abad, are 142, 183, and 218 mm, respectively. Note that modeling in artificial intelligence methods uses the available data and, as can be observed, the values obtained from artificial intelligence methods are generally lower than for the synoptic method. As can be seen, artificial neural network modeling achieved a better response for both precipitation and run-off data. Furthermore, based on the structure of this network established through use of artificial intelligence. Usage of this method alongside synoptic method allows us to investigate the basin as optimally as possible. Generally, artificial neural network methods, if the time data are well-distributed and we have a long time series, offer a suitable response to calculations.

Conclusion

Modeling hydrological processes is crucial for proper management of water resources, and since precipitation is of utmost importance because it is one of the main sources of water for drinking, industrial, and agricultural purposes, proper prediction of the course of precipitation and its effect on the runoff process contributes to better planning. In this study, three rain-gauge stations in the Tehran region were used to predict precipitation. This region is quite important because it serves as a base for industry and agriculture and is experiencing significant population growth. This region is located in a mountainous area, with a mean precipitation of 150 mm in the northern domains of Tehran and a precipitation of less than 150 mm in the southern domains, supporting a comprehensive investigation. Synoptic methods and isohyetal lines, followed by application of artificial neural network (ANN) methods, were used to model precipitation, and the results were investigated and compared.

The results of this research indicated that modeling by artificial neural network could offer a suitable response for predicting precipitation processes. In this regard, we observed a very high correlation coefficient of average 97%, quite acceptable for neural network studies. The results also showed that using synoptic methods combined with artificial network methods, one can predict and investigate precipitation in the best way. The Tehran region, because of its mountainous structure, is influenced by air masses from different regions, so for proper prediction, various factors should be considered. As in the synoptic method, if we apply an overhead rate, the precipitation values obtained using the synoptic method are generally larger than those obtained by the neural network; considering inclusion of mountain factors, it is even up to twice as large. Using the neural network method, we were able to investigate the basin over time, and the results obtained are not limited to maximum data. As is well-known, neural network methods are relatively weaker than field methods for estimating peak data.

References

Alvisi, S., Mascellani, G., Franchini, M., & Bardossy, A. (2006). Water level forecasting through fuzzy logic and artificial neural network approaches. *Hydrology and Earth System Sciences Discussions, 10*(1), 1-17.

Anctil, F., & Tape, D. G. (2004). An exploration of artificial neural network rainfall-runoff forecasting combined with wavelet decomposition. *Journal of Environmental Engineering and Science*, *3*(S1), S121-S128.

Chang, T. C., & Chao, R. J. (2006). Application of back-propagation networks in debris flow prediction. *Engineering Geology*, *85*(3-4), 270-280.

Daghighi, A., Nahvi, A., & Kim, U. (2017). Optimal Cultivation Pattern to Increase Revenue and Reduce Water Use: Application of Linear Programming to Arjan Plain in Fars Province. *Agriculture*, *7*(9), 73.

Daghighi, A.: Harmful Algae Bloom Prediction Model for Western Lake Erie Using Stepwise Multiple Regression and Genetic Programming, Electronic Thesis, available at: https://etd.ohiolink.edu/ (last access: 24 January 2019), 2017.

Danco, J. F., DeAngelis, A. M., Raney, B. K., & Broccoli, A. J. (2016). Effects of a warming climate on daily snowfall events in the northern hemisphere. *Journal of Climate*, *29*(17), 6295-6318.

Farajzadeh, J., Fard, A. F., & Lotfi, S. (2014). Modeling of monthly rainfall and runoff of Urmia lake basin using "feed-forward neural network" and "time series analysis" model. *Water Resources and Industry*, *7*, 38-48.

Haghiri, S., Daghighi, A., & Moharramzadeh, S. (2018). Optimum coagulant forecasting by modeling jar test experiments using ANNs. *Drinking Water Engineering and Science*, *11*(1), 1-8.

Hershfield, D. M. (1961). Estimating the probable maximum precipitation. *Journal of the hydraulics Division*, *87*(5), 99-116.

Hsu, K. L., Gupta, H. V., & Sorooshian, S. (1995). Artificial neural network modeling of the rainfall- runoff process. *Water resources research*, *31*(10), 2517-2530.

Kagan, A. M., Rao, C. R., & Linnik, Y. V. (1973). Characterization problems in mathematical statistics.

Ketabchy, M., Sample, D. J., Wynn-Thompson, T., & Yazdi, M. N. (2018). Thermal evaluation of urbanization using a hybrid approach. *Journal of environmental management*, *226*, 457-475.

Kisi, O., Shiri, J., & Tombul, M. (2013). Modeling rainfall-runoff process using soft computing techniques. *Computers & Geosciences*, *51*, 108-117.

Legates, D. R., & McCabe Jr, G. J. (1999). Evaluating the use of "goodness- of- fit" measures in hydrologic and hydroclimatic model validation. *Water resources research*, *35*(1), 233-241.

Mahmoudpour, M., Khamehchiyan, M., Nikudel, M. R., & Ghassemi, M. R. (2016). Numerical simulation and prediction of regional land subsidence caused by groundwater exploitation in the southwest plain of Tehran, Iran. *Engineering Geology*, *201*, 6-28.

Mishra, A. K., & Desai, V. R. (2006). Drought forecasting using feed-forward recursive neural network. *ecological modelling*, *198*(1-2), 127-138.

Nahvi, A., Daghighi, A., & Nazif, S. (2018). The environmental impact assessment of drainage systems: a case study of the Karun river sugarcane development project. *Archives of Agronomy and Soil Science*, *64*(2), 185-195.

Nikoo, M. R., Gavahi, K., & Khoramshokooh, N. (2017). A Multi-objective Simulation–Optimization Approach for Design of Cutoff Walls and Apron of Diversion Dams. *Iranian Journal of Science and Technology, Transactions of Civil Engineering*, 1-12.

Partal, T., & Kişi, Ö. (2007). Wavelet and neuro-fuzzy conjunction model for precipitation forecasting. *Journal of Hydrology*, *342*(1-2), 199-212.

Pradhan, B., & Lee, S. (2010). Regional landslide susceptibility analysis using back-propagation neural network model at Cameron Highland, Malaysia. *Landslides*, *7*(1), 13-30.

Rajaee, T., Nourani, V., Zounemat-Kermani, M., & Kisi, O. (2010). River suspended sediment load prediction: application of ANN and wavelet conjunction model. *Journal of Hydrologic Engineering*, *16*(8), 613-627.

Rosso, O. A., Karakas, S., & Cakmak, E. D. (2006, September). Wavelet-based informational tools in the analysis of early gamma response. *In international journal of psychophysiology*, vol. 61, no. 3, pp. 324-324.

Tokar, A. S., & Johnson, P. A. (1999). Rainfall-runoff modeling using artificial neural networks. *Journal of Hydrologic Engineering*, *4*(3), 232-239.

Yazdi, M. N., Arhami, M., Ketabchy, M., & Delavarrafeei, M. (2016). Modeling of Cement Factory Air Pollution Dispersion by AERMOD.

Zodrow, K. R., Li, Q., Buono, R. M., Chen, W., Daigger, G., Dueñas-Osorio, L., ... & Logan, B. E. (2017). Advanced materials, technologies, and complex systems analyses: Emerging opportunities to enhance urban water security.